EUROPEAN ORGANIZATION FOR NUCLEAR RESEARCH

CERN-SPSC-2011-001
SPSC-P-284 Add. 5
February 9, 2011

SEARCH FOR LONG-LIVED STATES OF $\pi^+\pi^-$ ATOMS

Addendum to the DIRAC Proposal

B.Adeva[n], L.Afanasyev[k], C.Amsler[p], A.Anania[f], S.Aogaki[h], K.Augsten[b], A.Benelli[p], V.Brekhovskikh[m], T.Cechak[b], M.Chiba[i], C.Ciortea[j], C.Ciocarlan[j], S.Constantinescu[j], C.Curceanu[e], P.Doškářová[b], A.Dudarev[k], D.Dumitriu[j], D.Drijard[a], A.Enulescu[j], D.Fluerasu[j], O.Gortchakov[k], K.Gritsay[k], C.Guaraldo[e], M.Gugiu[j] M.Hansroul[a], R.Hosek[b], Z.Hons[d], V.Karpukhin[k], J.Kluson̆[b], M.Kobayashi[g], A.Kulikov[k], E.Kulish[k], A.Kuptsov[k], V.Kruglov[k], L.Kruglova[k], K.-I.Kuroda[k], A.Lamberto[f], R.Lednicky[c], J.Martinčik[b], L.Nemenov[k], M.Nikitin[k], K.Okada[h], M.Pentia[j], M.Plo[n], P.Prusa[b], G.F.Rappazzo[f], A.Ryazantsev[m], A.Romero Vidal[e], V.Ronzhin[m], V.Rykalin[m], J.Saborido[n], J.Schacher[o], P.Shlyapnikov[m], J.Smolík[b], F.Takeutchi[h], A.Tarasov[k], T.Trojek[b] T.Urban[b] T.Vrba[b] P.Vázquez[n], V.Yazkov[l], Y.Yoshimura[g], M.Zhabitsky[k], P.Zrelov[k]

[a] CERN, Geneva, Switzerland
[b] Czech Technical University, Prague, Czech Republic
[c] Institute of Physics ASCR, Prague, Czech Republic
[d] Nuclear Physics Institute ASCR, Rez, Czech Republic
[e] INFN - Laboratori Nazionali di Frascati, Frascati, Italy
[f] Messina University and INFN-Messina, Italy
[g] KEK, Tsukuba, Japan
[h] Kyoto Sangyou University, Japan
[i] Tokyo Metropolitan University, Japan
[j] National Institute for Physics and Nuclear Engineering IFIN-HH, Bucharest, Romania
[k] JINR Dubna, Russia
[l] Skobeltsyn Institute for Nuclear Physics of Moscow State University
[m] IHEP Protvino, Russia
[n] Santiago de Compostela University, Spain
[o] Bern University, Switzerland
[p] Zurich University, Switzerland

GENEVA
2011

Abstract

The proposed experiment is a further development of the DIRAC experiment already running at CERN PS. Up to now more than 21000 $\pi^+\pi^-$ pairs originated from the $\pi^+\pi^-$ atom ($A_{2\pi}$) breakup were identified and the overall accuracy of the $A_{2\pi}$ lifetime is about 9% in accordance with the DIRAC proposal. This measurement allowed to extract the difference $|a_0 - a_2|$ of s-wave $\pi\pi$-scattering length with accuracy of 4.3%.

The observation of long-lived (metastable) $A_{2\pi}$ states will be performed with the same setup. This observation opens a possibility to measure the energy difference between ns and np states and to determine the value of another combination $2a_0 + a_2$ of $\pi\pi$ scattering length in a model-independent way. In combination with the first measurement it allows to get a_0 and a_2 separately.

An additional measurement of the multiple scattering angles in different materials with accuracy better than 1% will be performed in parallel with the observation. This measurement is needed to improve the systematic accuracy in the $A_{2\pi}$ lifetime for the data already collected in 2008–2010.

Contents

1 Physics motivation

The decay probability of $\pi^+\pi^-$ atoms ($A_{2\pi}$) is dominated by the annihilation process

$$\pi^+ + \pi^- \to \pi^0 + \pi^0 \tag{1}$$

(branching ~ 99.6%) and depends on the difference between the s-wave $\pi\pi$ scattering lengths with isospins zero (a_0) and two (a_2) [URET61, BILE69, JALL98, IVAN98].

$$\frac{1}{\tau} \approx W_{\pi^0\pi^0} = R\,|a_0 - a_2|^2\,. \tag{2}$$

The most accurate ratio of $W_{\pi^0\pi^0}$ to the square of $\pi\pi$ scattering length difference $|a_0 - a_2|$ was derived in [GASS01]: R has been obtained within 1.2% accuracy.

In order to get values of a_0 and a_2 separately from $\pi^+\pi^-$ atom data, one may exploit the fact that the energy splitting between the levels ns and np, $\Delta E_n = E_{ns} - E_{np}$, depends on another combination of the scattering lengths: $2a_0 + a_2$ [EFIM86]. In the πN case this dependence of the atomic level shift on scattering lengths in the s-states has been derived in [DESE54]. The influence of the strong and electromagnetic interactions on the $A_{2\pi}$ energy structure was studied in [KARI79, AUST83, EFIM86, GASH98, EIRA00]. An elaborated analysis of the $A_{2\pi}$ energy structure was performed in [SCHW04].

The energy shift for the levels with the principal quantum number n and orbital quantum number l comprises few contributions:

$$\Delta E_{nl} = \Delta E^{\rm em}_{nl} + \Delta E^{\rm vac}_{nl} + \Delta E^{\rm str}_{nl}, \tag{3}$$

where $\Delta E^{\rm em}_{nl}$ includes relativistic insertions, finite-size effect, self-energy corrections due to transverse photons and transverse photon exchange. The term $\Delta E^{\rm vac}_{nl}$ includes the contributions from the vacuum polarization. The last term $\Delta E^{\rm str}_{nl}$ takes into account strong interaction effects and is related to the $\pi\pi$ scattering lengths as follows:

$$\Delta E^{\rm str}_{n0} = A_n(2a_0 + a_2). \tag{4}$$

For the ground state the coefficient A_1 is know within 2.1% [SCHW04]. The values of the energy shifts for the levels with $n = 1$ and 2 are presented in Table 1. Hence, the theoretical value for the 2s − 2p

Table 1: *Numerical values for the energy shift [SCHW04]*

	$\Delta E^{\rm em}_{nl}$(eV)	$\Delta E^{\rm vac}_{nl}$(eV)	$\Delta E^{\rm str}_{nl}$(eV)
$n=1,\ l=0$	-0.065	-0.942	$-3.80 \pm .1$
$n=2,\ l=0$	-0.012	-0.111	-0.47 ± 0.01
$n=2,\ l=1$	-0.004	-0.004	$\simeq -1\times10^{-6}$

energy splitting is given by

$$\Delta E^{\rm 2s-2p} = \Delta E^{\rm str}_{20} + \Delta E^{\rm em}_{20} - \Delta E^{\rm em}_{21} + \Delta E^{\rm vac}_{20} - \Delta E^{\rm vac}_{21} = -0.59 \pm 0.01{\rm eV}. \tag{5}$$

By measuring the value of $\Delta E_n = \Delta E^{n{\rm s}-n{\rm p}}$ one can determine the numerical value of $\Delta E^{\rm str}_{n0}$, as all other terms in Eq. (3) have been calculated with a high accuracy. From (5) and Table 1 it follows that the strong interaction effects contributes up to 80% of the full energy shift. This fact provides a high sensitivity of a $\Delta E^{\rm 2s-2p}$ measurement to the value of the term $2a_0 + a_2$. Thus, measurements of the energy shift ΔE_n make it possible to obtain values for the new combination of scattering lengths $2a_0 + a_2$ in a model-independent way.

The most accurate theoretical predictions for the s-wave $\pi\pi$ scattering lengths have been achieved by [COLA01B] (in units $M^{-1}_{\pi^+}$):

$$a_0 = 0.220 \pm 2.3\%\,, \quad a_2 = -0.0444 \pm 2.3\%\,, \quad a_0 - a_2 = 0.265 \pm 1.5\%\,. \tag{6}$$

The best experimental results obtained by NA48/2 from investigating the K_{e4} decay [NA48-10] are the following ones:

$$\begin{aligned} a_0 &= 0.2220 \pm 0.0128_{\text{stat}} \pm 0.0050_{\text{syst}} \pm 0.0037_{\text{theo}} \\ a_2 &= -0.0432 \pm 0.0086_{\text{stat}} \pm 0.0034\text{syst} \pm 0.0028_{\text{theo}} \end{aligned} \tag{7}$$

From the analysis of the decay $K^{\pm} \to \pi^{\pm}\pi^0\pi^0$ the same experiment obtained [NA48-09]

$$\begin{aligned} a_0 - a_2 &= 0.2571 \pm 0.0048_{\text{stat}} \pm 0.0025_{\text{syst}} \pm 0.0014_{\text{ext}} \\ a_2 &= -0.024 \pm 0.013_{\text{stat}} \pm 0.009\text{syst} \pm 0.002_{\text{ext}} \end{aligned} \tag{8}$$

These are also addional theorectical uncertainties of 0.0088 for $a_0 - a_2$ and of 0.015 for a_2.

The result of DIRAC basing on 21000 observed atoms collected in 2000–2003 [ADEVA11] is

$$|a_0 - a_2| = 0.2533^{+0.0080}_{-0.0078}(\text{stat})^{+0.0077}_{-0.0072}(\text{sys}) = \ldots \pm 4.3\%_{\text{tot}}. \tag{9}$$

2 Study of long-lived states as a method for energy shift measurement

The method for measuring ΔE_n was qualitatively discussed in [NEME85]. By studying the dependence of the $A_{2\pi}$ long-lived state ($l \geq 1$) lifetime on the applied electric field, it is possible to extract an experimental value for ΔE^{ns-np} [NEME85, NEME01, NEME02].

In inclusive processes $A_{2\pi}$ are produced in s-states distributed over the principal quantum number n proportional to n^{-3}. When moving inside the target, the relativistic $A_{2\pi}$ interacts with the electric field of the target atoms and with some probability will leave the target with orbital momentum $l \neq 0$. Calculations show that up to $\sim 10\%$ of the atoms, generated in a thin target, reach the vacuum region in a long-lived state [AFAN97]. The main part of these atoms will be in the 2p-state. For $A_{2\pi}$ in p-state the decay into two π^0-mesons is forbidden by the conservation law for the angular momentum, and the process $A_{2\pi} \to \pi^0 + \gamma$ is also strongly suppressed. Therefore, the main mechanism of the 2p-state decay is the 2p–1s radiative transition with a subsequent annihilation from 1s-state into two π^0 with the lifetime of $\tau_{1s} \approx 3 \times 10^{-15}$ s. Thus, the lifetime of the atom in the 2p-state is determined by the radiative transition probability equivalent to $\tau_{2p} = 1.17 \times 10^{-11}$ s [NEME85]. For the average $A_{2\pi}$ momentum in DIRAC of 4.5 GeV/c ($\gamma = 16.1$) the corresponding decay length is 5.7 cm for $2p$-state , 19 cmfor $3p$ and 43 cm for $4p$.

The $A_{2\pi}$ decay from ns-states is allowed with the corresponding lifetimes $\tau_{ns} = \tau_{1s} n^3$. Since the lifetime in np-states is about 10^3 of the ns-state lifetime, it is possible to measure the energy difference of these levels by exerting an electrical field on the atom by tracking the field dependence of the decay probability, due to the mixing of ns- and np-states in the external electrical field.

In [NEME01] the influence of constant magnetic field on the $A_{2\pi}$ atom lifetime was studied, and the possibility was demonstrated for measuring the splitting between $2s$ and $2p$ levels with the use of relativistic atomic beams produced in existing accelerators.

The transverse magnetic field B_0 in the lab reference frame is increased in its amplitude in the atom reference frame and is equal to $B = \gamma B_0$ (γ is Lorentz factor). The corresponding electric field has nearly the same amplitude $F = \beta B$ (β is the atom velocity in the lab frame) and is perpendicular to the atom momentum. In the electric field a small admixture of the $2s$-state to the $2p$-state wave function arises. This admixture may cause a significantly faster decay for atoms initially being in the $2p$-state. For the case of $B_0 = 4$ T and $\gamma = 20$, the decay rate increases more than twice.

Another possibility to measure the energy shift ΔE_n is to use the resonance method [NEME02] which allows to achieve a higher accuracy.

Similar approach to the energy shift measurement can be applied to the $\pi^{\pm}K^{\mp}$ atoms. The energy difference between the $2s$ and $2p$ πK-atomic levels consists of two electromagnetic components, $\Delta E^{em}_{2s-2p} = -0.013$ eV and $\Delta E^{vac}_{2s-2p} = -0.27$ eV, and a strong component, $\Delta E^{\rm str}_{2s-2p} \propto (2a_0^{1/2} + a_0^{3/2})$ (see ref. [SCHW04]). By inserting the πK scattering lengths from [BUTT04] in the above equation, one gets $\Delta E^{\rm str}_{2s-2p} = (-1.1 \pm 0.1)$ eV [SCHW04], yielding in total the 2s−2p energy splitting $\Delta E^{\rm 2s-2p} = -1.4 \pm 0.1$ eV. The strong part $\Delta E^{\rm str}_{2s-2p}$ of this splitting is - in principle - measurable [NEME85]. The quantity $2a_0^{1/2} + a_0^{3/2}$ as described in Chiral Perturbation Theory (ChPT) involves a combination of low energy constants, $2L_6 + L_8$, which provides information on the quark condensate and the strange to non-strange quark mass ratio [DESC03].

3 Yields of $A_{2\pi}$ long-lived states

To obtain numerical values for the $A_{2\pi}$ long-lived state production we chose the approach, in which the evolution of the atomic state population is described in terms of probabilities. For the values below, the $A_{2\pi}$ ground-state lifetime was fixed to 3.0×10^{-15} s and the atom momentum to 4.5 GeV/c. Note that the results are essentially independent on these parameter values.

The yields of $\pi^+\pi^-$ atoms in np states has been considered for different target materials and thicknesses with the intention to optimize the experimental conditions for their observation [AFAN05]. Aiming this goal, for few materials the yields of long-lived atoms $A^l_{2\pi}$ were calculated as a function of target thickness and atoms quantum numbers. The results of this calculation are presented for Be, Ni, and Pt targets (see Figs. 1, 2, 3, 4). From the analysis of these distributions the target thicknesses which give the maximum yield of $A^l_{2\pi}$ were found .

It is shown that for DIRAC thinner targets with smaller Z provide a higher yield of np states and a better ratio to the atom breakup. Table 2 presents a set of targets providing highest yield of the long-lived states with orbital quantum numbers $l \geq 1$. Also shown are the yields of p-states with the magnetic quantum number $m = 0$ ($2p_0$, $3p_0$, $4p_0$). In electric fields these states can be mixed with s-states and thus are suitable for energy shift measurements.

Table 2: *For different target materials with atomic number Z the following values are shown: probability of $A_{2\pi}$ breakup, total yield of long-lived states $\sum(l \geq 1)$ including states with $n \leq 7$, yields of p-states with magnetic quantum number $m = 0$ ($2p_0$, $3p_0$, $4p_0$) and their sum $\sum(l = 1, m = 0)$ up to $n = 7$. The target thicknesses were chosen in order to provide maximum yield of long-lived states.*

Target Z	Thickness μm	Breakup	$\sum(l \geq 1)$	$2p_0$	$3p_0$	$4p_0$	$\sum(l = 1, m = 0)$
Be 04	100	6.3%	5.5%	1.18%	0.46%	0.15%	1.90%
Ni 28	5	9.42%	9.69%	2.40%	0.58%	0.18%	3.29%
Pt 78	2	18.8%	10.5%	2.70%	0.55%	0.16%	3.53%

All results presented in table 2 were obtained for the $A_{2\pi}$ momentum $P_{\rm A} = 4.5$ GeV/c. Figure 4 shows that the $A_{2\pi}$ yield for the 5 μm thin target has only a weak dependence on $P_{\rm A}$ in the setup momentum range (2.6 $GeV/c \leq P_{\rm A} \leq 8$ GeV/c).

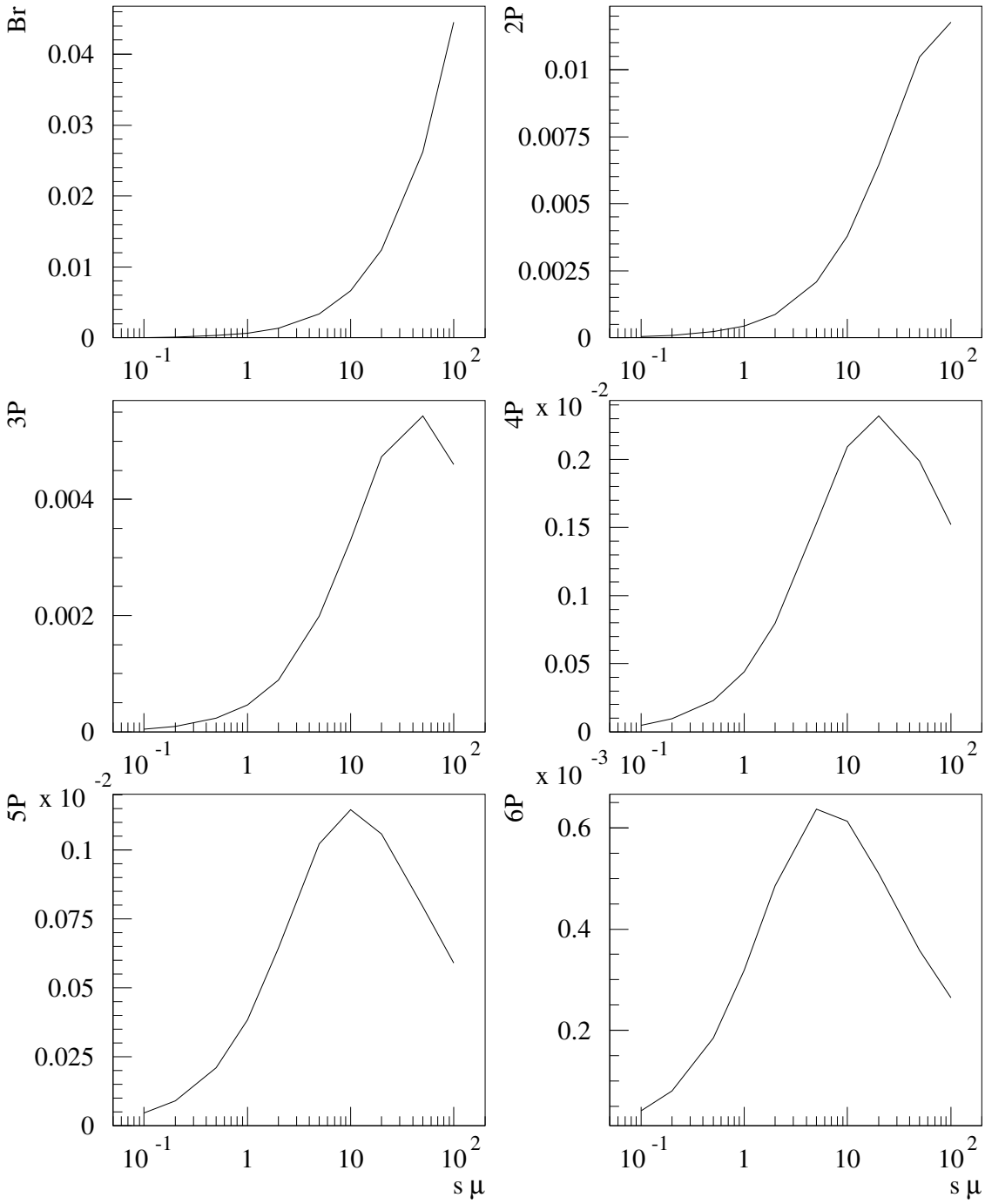

Figure 1: *Probabilities of the $A_{2\pi}$ breakup (Br) and yields of the long-lived states $2p$, $3p$, $4p$, $5p$, $6p$ ($m = 0$) as a function of the Beryllium ($Z = 4$) target thickness. The $A_{2\pi}$ ground state lifetime is assumed to be $3.0 \cdot 10^{-15}$ s and the atom momentum 4.5 GeV/c.*

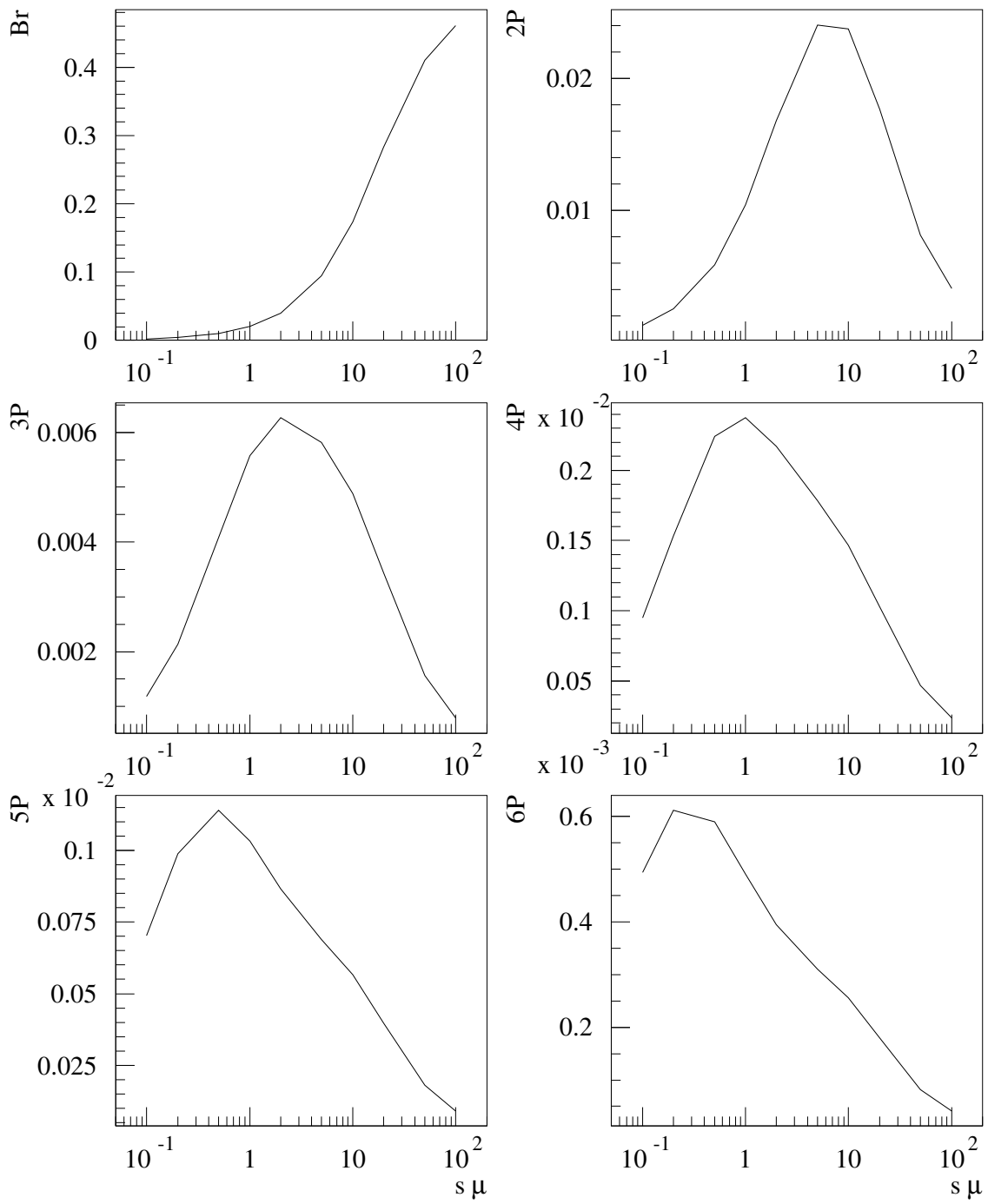

Figure 2: *Probabilities of the $A_{2\pi}$ breakup (Br) and yields of the long-lived states $2p$, $3p$, $4p$, $5p$, $6p$ ($m = 0$) as a function of the Nickel ($Z = 28$) target thickness. The $A_{2\pi}$ ground state lifetime is assumed to be $3.0 \cdot 10^{-15}$ s and the atom momentum 4.5 GeV/c.*

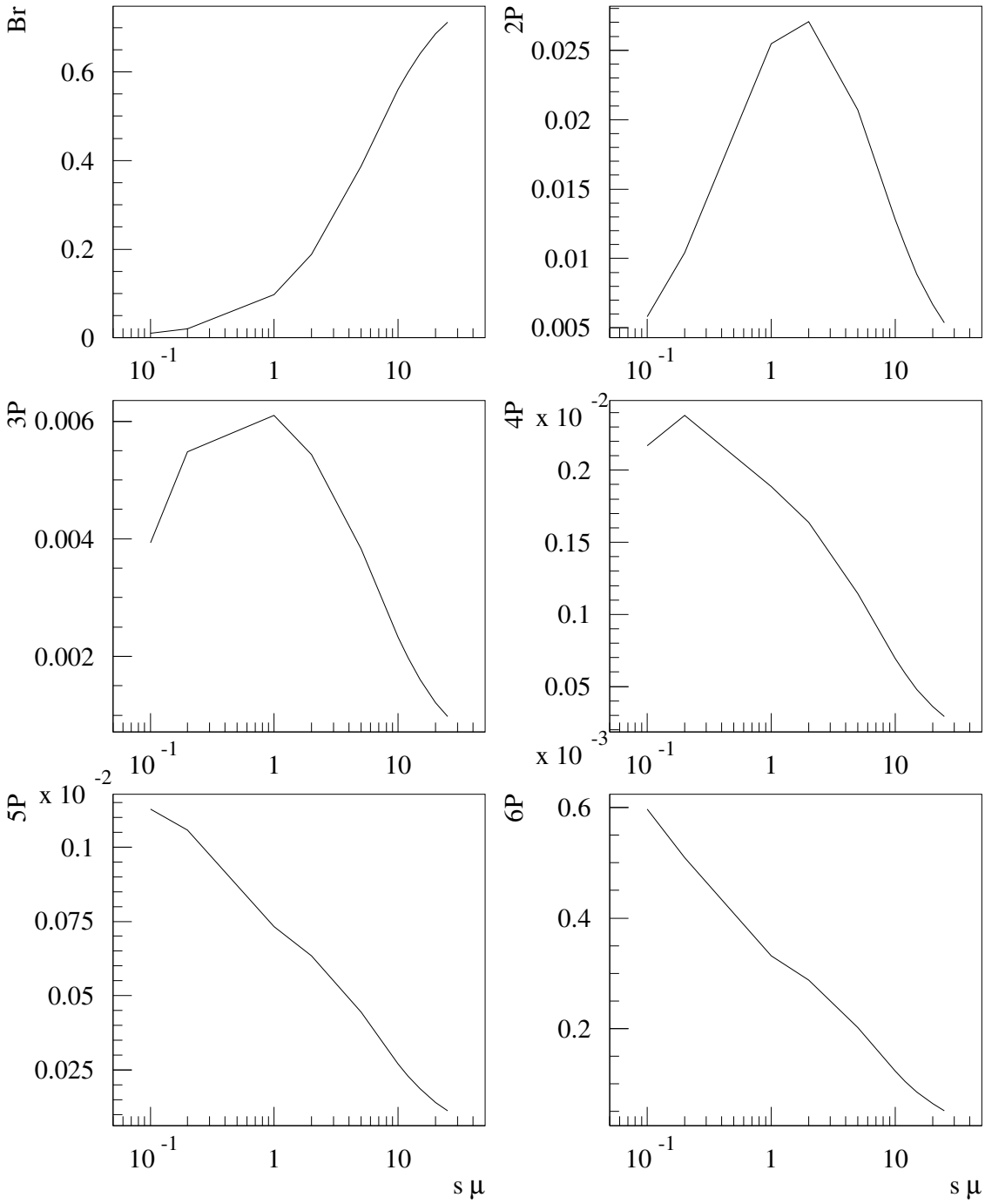

Figure 3: *Probabilities of the $A_{2\pi}$ breakup (Br) and yields of the long-lived states $2p$, $3p$, $4p$, $5p$, $6p$ ($m = 0$) as a function of the Platinum ($Z = 78$) target thickness. The $A_{2\pi}$ ground state lifetime is assumed to be $3.0 \cdot 10^{-15}$ s and the atom momentum 4.5 GeV/c.*

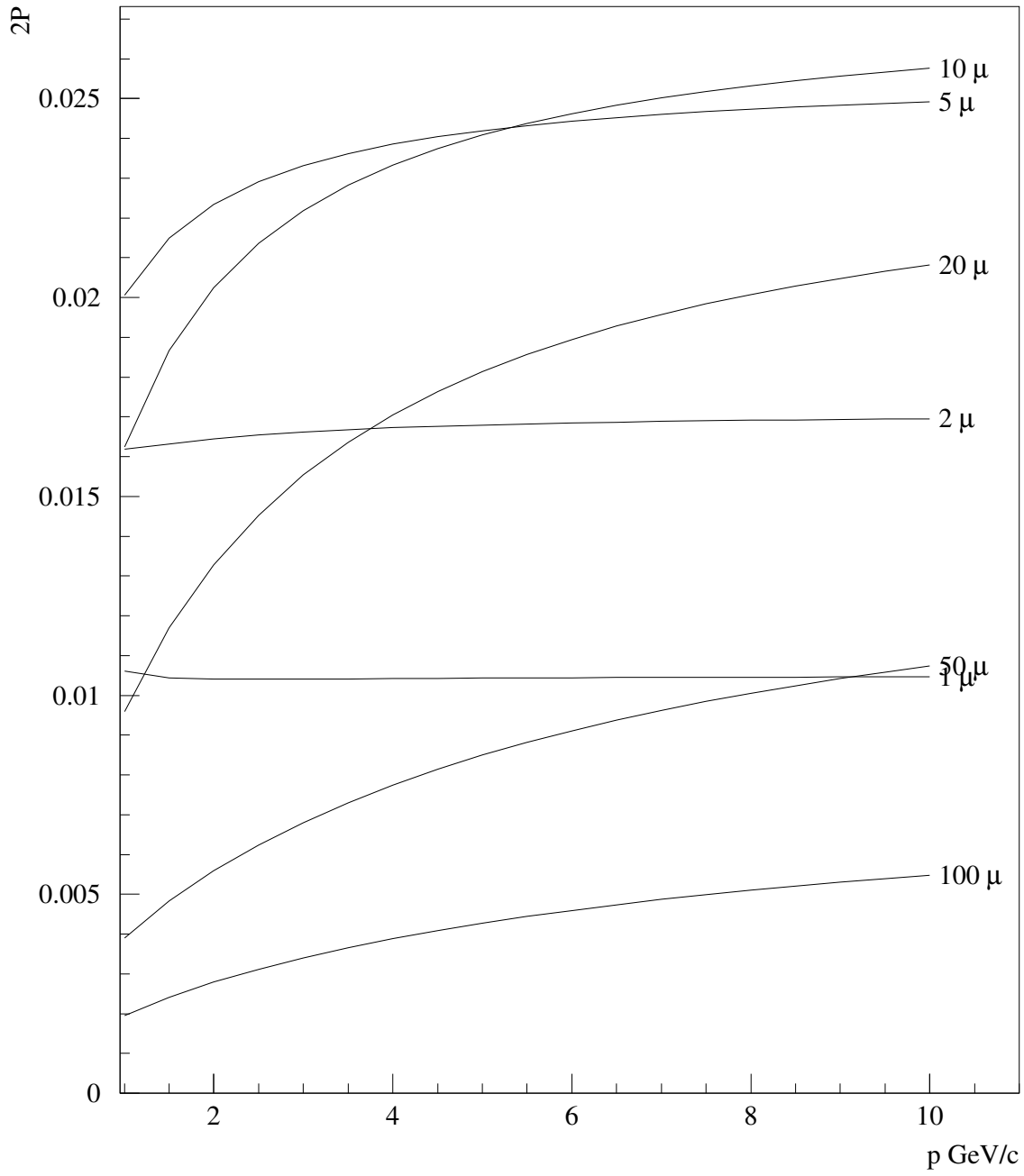

Figure 4: *Yields of the long-lived states* $2p$ $(m = 0)$ *of* $A_{2\pi}$ *as a function of the atom momentum for the Nickel* $(Z = 28)$ *targets. Target thicknesses are given in microns on the right side of the picture. The* $A_{2\pi}$ *ground state lifetime was assumed to be* $3.0 \cdot 10^{-15}$ *s.*

4 Generating $A_{2\pi}$ in long-lived states on Beryllium

Up to now DIRAC (see Fig. 5) took data with a Nickel target of 100 μm thickness providing the best sensitivity in the $A_{2\pi}$ lifetime measurement. To get the maximum yield of the long-lived states the thickness of Ni target need to be reduced to 5 μm, that requires increase of the beam intensity by a factor of 20 in order to obtain the same number of proton-target interactions. However it can not be realized for a variety of reasons: accelerator limits, radio-protection restrictions, overloading of a major part of detectors and so on. For this reason the target material need to be replaced by one having a higher nuclear efficiency.

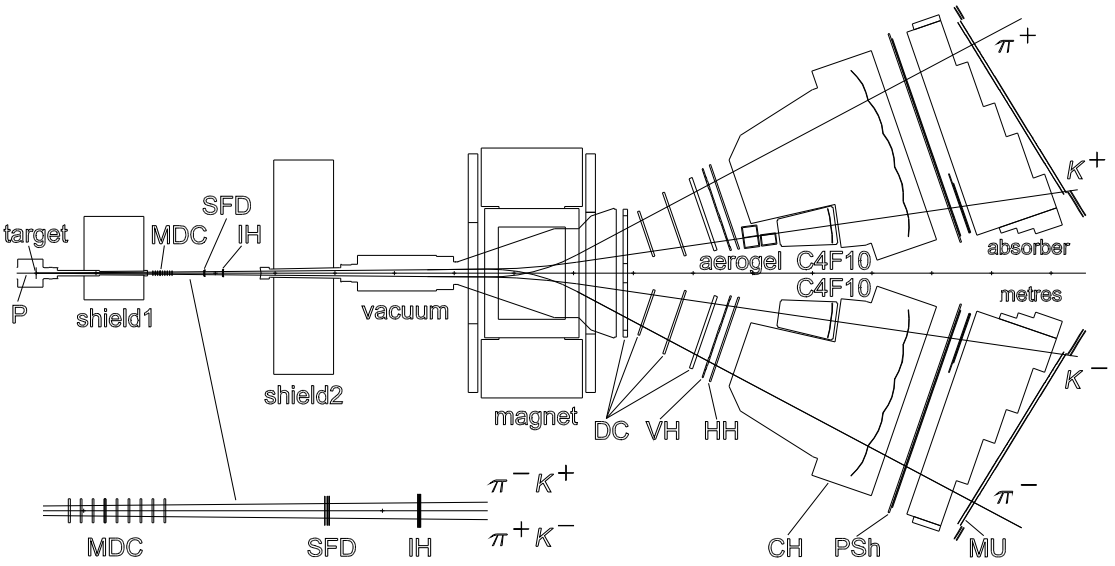

Figure 5: *DIRAC setup: MDC are microdrift gas chambers, SFD is a scintillating fiber detector and IH is a scintillation ionization hodoscope. Downstream the spectrometer magnet there are drift chambers (DC), vertical (VH) and horizontal (HH) scintillation hodoscopes, Cherenkov detectors containing nitrogen (CH), heavy gas C4F10 and aerogel radiators, shower detectors (PSh) and scintillation muon detectors (MU).*

For a 100 μm Beryllium target the nuclear efficiency ε_{nucl} is 7 times larger than for 5 μm Ni (see Table 3). Therefore the proton beam intensity must be only about 3 times larger in order to get the needed number of primary interactions.

Table 3: *Target thickness L in micron, in radiation length (X/X_0), and nuclear efficiency (probability for proton-nucleus interaction).*

	Be	Al	Ni	Pt
L(μm)	100	20	5	2
$\frac{X}{X_0} \times 10^4$	2.84	2.24	3.53	6.57
$\varepsilon_{nucl} \times 10^4$	2.45	0.48	0.34	0.23

The proton-target beam interaction will generate $A_{2\pi}$ in ns states as follows:

$$W_{1s} = 83\%, W_{2s} = 10.4\%, W_{3s} = 3.1\%, W_{>3s} = 3.5\%.$$

Passing through the target, a part of $A_{2\pi}$ interacts with Be-atoms and hence will be excited into $2p, 3p, 4p, ...$ states (see Figure 6). The main excitation processes are $1s \to np$ transitions.

For 100 μm Be about 5.5% long-lived atoms $A^l_{2\pi}$ (Table 2) escape the target and enter into the vacuum part of the secondary particle channel. All atoms will annihilate at a distance about 150 cm. While the short-lived states will annihilate in the target or near the target at a distance of less than 2 mm (Figure 6). The decay lengths of $A_{2\pi}$ with $\gamma = 20$ in $1s, 2s, 3s$ and $4s$ states are 0.017 mm, 0.14 mm, 0.46 mm and 1.1 mm. About 6.3% of the $A_{2\pi}$ atoms will break up in the target, producing $n_{\rm A}^{\rm Be}$ atomic pairs having $Q_T \leq 1.5$ MeV/c. The quantity Q_T is the transverse component of the relative momentum Q in the atomic pair c.m.s.

The proton beam interacting with the target can produce also Coulomb ($N_{\rm C}^{\rm Be}$) and non-Coulomb pairs ($N_{\rm nC}^{\rm Be}$). These pairs are detected by the setup and represent the main background causing the main part of the errors in $n_{\rm A}^{\rm Be}$ and $N_{\rm A}^{\rm Be}$, where $N_{\rm A}$ is the full number of produced atoms.

By analyzing experimental distributions of $\pi^+\pi^-$ pairs in Q_T and Q_L one can obtain the amount of Coulomb and non-Coulomb pairs. The number of Coulomb pairs with small Q ($Q \leq 3$ MeV/c) allows one to calculate the number of produced atoms $N_{\rm A}$, using precise ($\leq 1\%$) formula and the expected number of atomic pairs $n_{\rm A}^{\rm Be}$ (see for example [ADEV05]).

Knowing the $A_{2\pi}$ ground state lifetime, the theory of $A_{2\pi}$ interaction with other atoms and the description of their propagation through the target (precision $\leq 1\%$) allow to calculate the number of $A_{2\pi}$ produced in Be in long-lived states $N^l_{\rm A}(Be)$ and $n_{\rm A}^{\rm Be}$ and the corresponding distribution in Q, Q_T and Q_L. The value $n_{\rm A}^{\rm Be}$ can also be extracted from the experiment by subtracting the Coulomb and non-Coulomb pair background.

5 Detecting $A_{2\pi}$ in long-lived states with a thin Platinum foil

Placing a 1 or 2 μm thin Pt foil behind the Be target, the largest part of long-lived atoms, $N^l_{\rm A}$, will break up, providing an additional number of atomic pairs, $n^l_{\rm A}$ (see Figure 6). Table 4 presents the atom breakup probability as a function of target thickness and $A_{2\pi}$ quantum numbers.

Table 4: *Breakup probability for np states and different thicknesses of Platinum foils. ($A_{2\pi}$ momentum $P_{\rm A} = 4.5\,GeV/c$ and $A_{2\pi}$ lifetime $\tau = 3\times10^{-15}s$)*

Thickness (μm)	2p	3p	4p	5p	6p	7p
0.1	0.0251	0.0520	0.0858	0.1327	0.2035	0.3219
0.2	0.0559	0.1175	0.1978	0.3001	0.4185	0.5392
0.5	0.1784	0.3595	0.5537	0.7176	0.8323	0.9043
1.0	0.4147	0.6895	0.8553	0.9324	0.9667	0.9828
1.5	0.6084	0.8526	0.9446	0.9765	0.9889	0.9944
2.0	0.7422	0.9244	0.9743	0.9895	0.9951	0.9975
3.0	0.8844	0.9739	0.9918	0.9967	0.9985	0.9992
4.0	0.9415	0.9882	0.9964	0.9986	0.9993	0.9997
5.0	0.9651	0.9934	0.9980	0.9992	0.9996	0.9998
10.0	0.9862	0.9975	0.9993	0.9997	0.9999	0.9999

Using Table 2, Table 4 and simulation [DIPGEN] it is possible to calculate the effective breakup probability, W_{br} for the atomic pairs created by the $A^l_{2\pi}$ breakup and their distribution on relative momentum Q. For the thickness of 2 μm $W_{br} = 0.82$. About 95% of the atomic pairs have $0 \leq Q_T \leq 1.$ MeV/c. If the foil were thicker, then the upper limit of Q_T would increase, the number of background Coulomb pairs would also increase and hence the precision for the $n^l_{\rm A}$ measurement decreases.

The distance between the Be target and the Pt foil was chosen to be 100 mm for excluding interaction of the primary beam halo with the Pt foil.

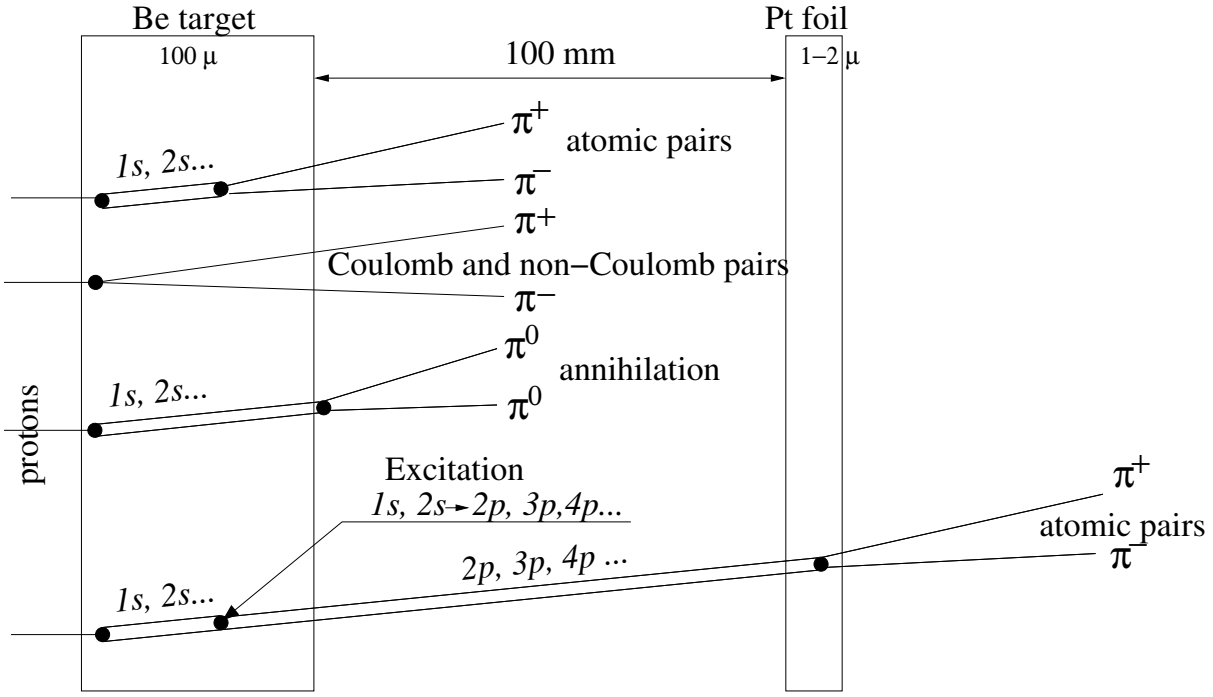

Figure 6: *Method to observe long-lived $A_{2\pi}$ by means of a breakup foil (Pt).*

6 Measurement of $A_{2\pi}$ production rate in p-Be interactions

During 7.5 days in August 2010 a small data sample was collected with 100 μm Beryllium target at intensity $2.6 \cdot 10^{11}$ proton per spill. This intensity was chosen to provide the same number of primary interactions in the target as in the usual working condition for Dirac during 2010, with the 100 μm Ni target and a $9.5 \cdot 10^{10}$ proton per spill intensity. The full proton flux through the target was $1.4 \cdot 10^{16}$. The measured multiplicity with Be in all detectors differs from the ordinary one by 2–3%. The single counts of all detectors increased in different scale for specific detectors: Ionization Hodoscope — 8%; Vertical Hodoscope positive arm — 3%, negative arm — 17%; Cherenkov counter for positrons — 25%, for electrons — 30%; Cherenkov counter for pions — 7% for both arms. The number of the first level triggers increased by 5%.

These data was analyzed in order to find the number of generated atoms using the standard analysis procedure for the DIRAC experiment [ADEV05]. There is a possibility to increase the efficiency of event reconstruction by a factor 1.2–1.5. Fig. 7 presents the distribution of experimental data (points with error bars) over the absolute value of Q_L for the events with $Q_T < 1$ MeV/c. The dashed line represents the fit of the experimental data with the sum of simulated “Coulomb" and “non Coulomb" data (see section 7) at the range $|Q_L| > 1$ MeV/c that eliminates the contribution of atomic pairs . The only free parameter in the fit is the fraction of “Coulomb pairs” respect to the “non-Coulomb” pairs, that results to be 0.18 . Using the known ratio of cross sections between $A_{2\pi}$ and “Coulomb pairs” [NEME85] and the experimentally measured number of Coulomb pairs, the number of generated atoms has been estimated :

$$N_A = 736 \pm 75 \tag{10}$$

Therefore, in a period of 6 months, equivalent to the one in 2010, it will be possible to collect the data sample which corresponds to 14000–15000 $A_{2\pi}$ generated in Beryllium target.

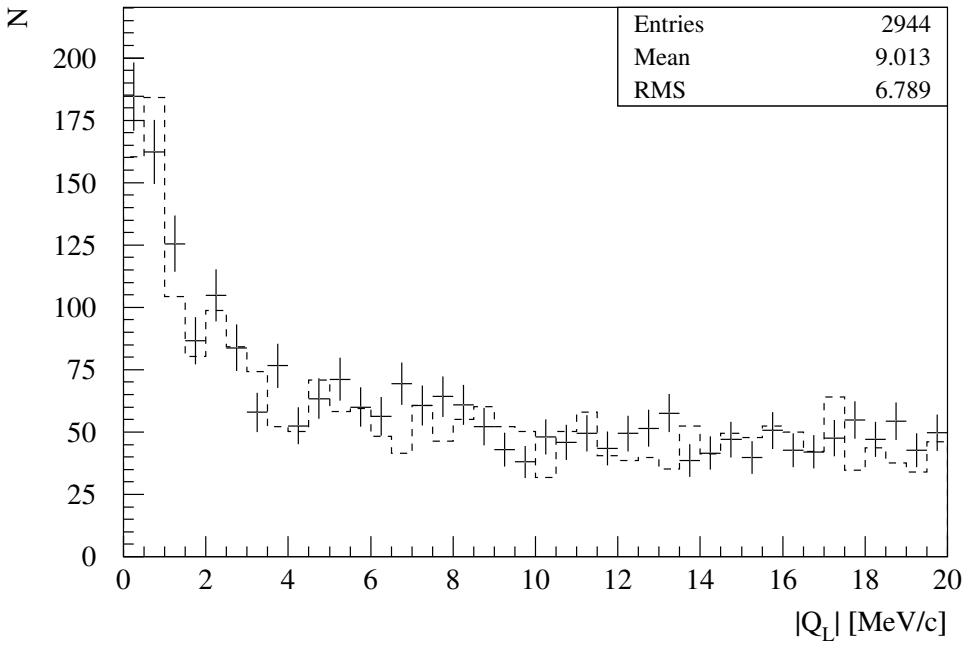

Figure 7: *Distribution of $\pi^+\pi^-$ pairs over $|Q_L|$ with the criterion $Q_T < 1$ MeV/c. Experimental data (points with error bars), collected in 2010 with Beryllium target, have been fitted by a sum of the simulated distribution of "Coulomb" and "non-Coulomb" pairs (dashed line).*

7 Simulation of all $\pi^+\pi^-$ pairs at experimental conditions

For the simulation of $\pi^+\pi^-$ pairs (atomic pairs, Coulomb and non-Coulomb pairs) the DIPGEN generator [DIPGEN] was used with some modifications describing interaction of the long-lived atoms with the additional Platinum foil. For the long-lived atoms the following processes were considered: production in the Beryllium target, their decay in the interval before the Platinum foil and breakup in the foil with production of atomic pairs.

In Tables 5 the relative population of $A_{2\pi}$ long-lived states are given at the exit of target and at the entry of foil. In Table 6 the numbers of atomic pairs produced in the 1 μm Pt foil from the states with specified n and l numbers are given. All numbers are normalized to the summed number in each table and are given in per mill.

Table 5: Pupulations of $A_{2\pi}$ long-lived states at the exit of target and at the entry of foil normalized to the summed number, given in ppm

at exit of target							
l \ n	2	3	4	5	6	7	8
1	417	148	48	18	7	3	1
2	0	117	49	20	9	4	1
3	0	0	45	21	10	4	2
4	0	0	0	20	10	5	2
5	0	0	0	0	10	5	2
6	0	0	0	0	0	4	2
7	0	0	0	0	0	0	2

at entry of foil							
l \ n	2	3	4	5	6	7	8
1	114	150	69	30	12	6	2
2	0	176	86	37	17	7	3
3	0	0	84	41	19	9	3
4	0	0	0	40	19	9	4
5	0	0	0	0	19	9	4
6	0	0	0	0	0	9	4
7	0	0	0	0	0	0	4

Table 6: The numbers of atomic pairs produced in the 1μm Pt foil from the states with specified n and l numbers normalized to the summed number, given in ppm.

l \ n	2	3	4	5	6	7	8
1	56	82	53	29	17	9	4
2	0	95	73	46	28	15	7
3	0	0	78	54	35	21	10
4	0	0	0	59	37	24	13
5	0	0	0	0	43	27	14
6	0	0	0	0	0	28	15
7	0	0	0	0	0	0	15

The lifetime of metastable atoms depends on their n and l values and this means that the relative population of different states varies in the interval between target and foil and their contribution to the total number of broken metastable atom depends of the distance between the target and foil. On Fig.8 and 9 the relative yields of atomic pairs produced in the Pt foil form the metastable atoms with different n and l (normalized on the total number of atoms produced in the Be target) are shown as a function of the distance between the Be target and Pt foil for the foils of 1 μm and 2 μm.

Then the pairs generated by the DIPGEN were transferred into GEANT-DIRAC (setup simulator) and ARIANE (reconstruction tool) programs. The distributions of reconstructed values of Q_L and Q_T for non-Coulomb, Coulomb pairs and pairs from metastable atoms are shown in Figs. 10 and 11.

At the target-foil distance of 100 mm the full probability of metastable atom breaking in the Pt foil of 1 μm is 0.81 and 0.94 for the foil of 2 μm.

To evaluate the metastable atom production as function of the Be target thickness some calculations were done keeping fixed the Be–Pt distance at 100 mm and the thickness of the Pt foil at 1 μm. The production of atoms decrease of 5.8% for thickness of 120μm and increases of 5.2% for the 80 μm Be target.

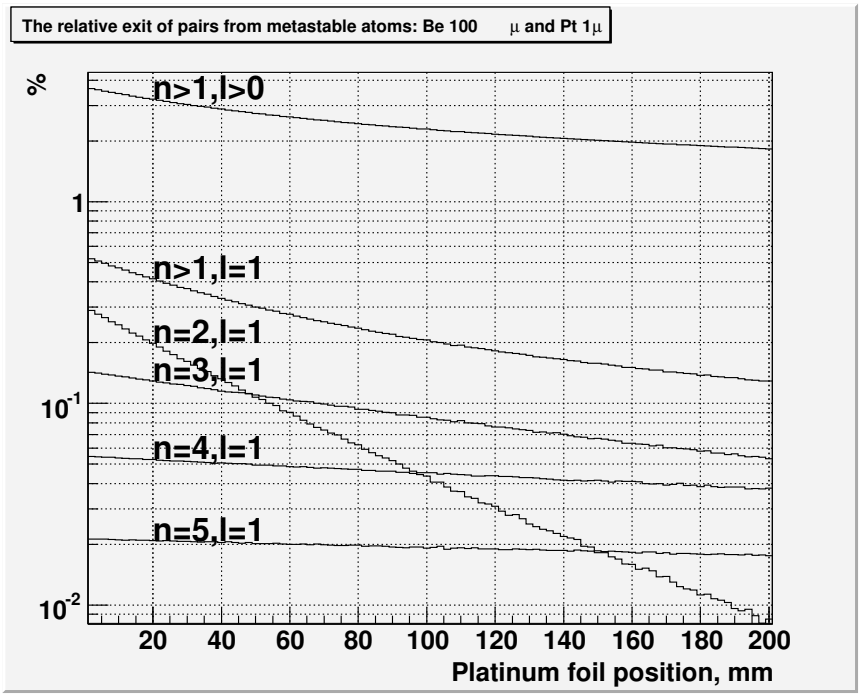

Figure 8: *Part of atoms where created in the Be target and then broken up in Pt foil in dependence on the distance between the target and foil for all metastable states ($n > 1, l > 0$) and for some individual states with $l = 1$. The foil thickness is 1 μ.*

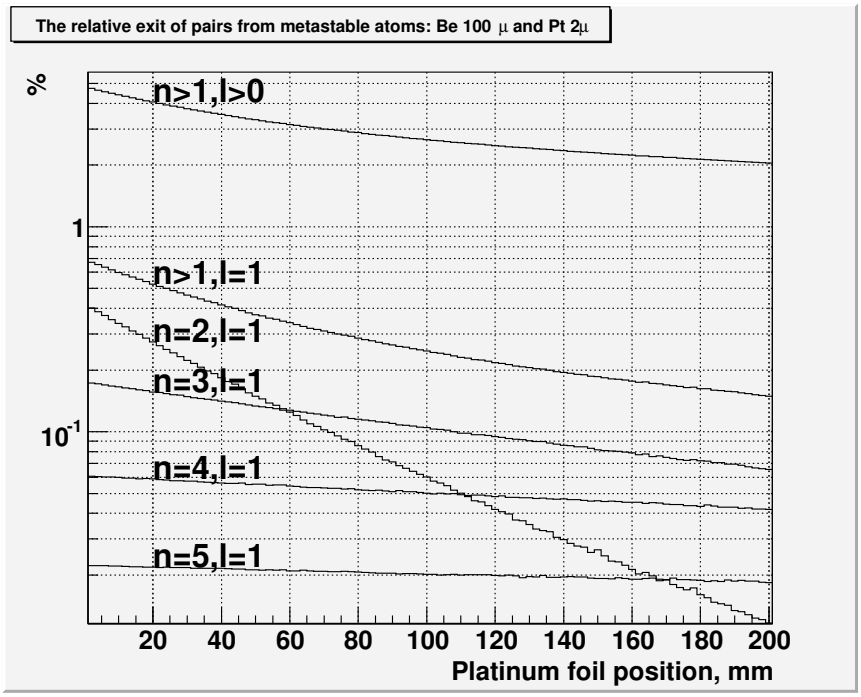

Figure 9: *Part of atoms where created in the Be target and then broken up in Pt foil in dependence on the distance between the target and foil for all metastable states ($n > 1, l > 0$) and for some individual states with $l = 1$. The foil thickness is 2 μ.*

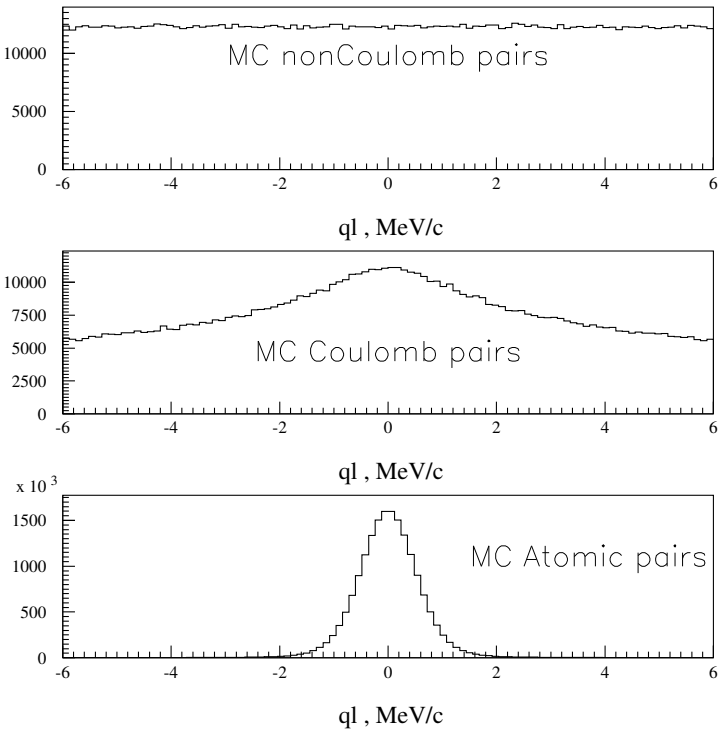

Figure 10: *Distributions of reconstructed values of Q_l for non-Coulomb, Coulomb pairs and pairs from metastable atom.*

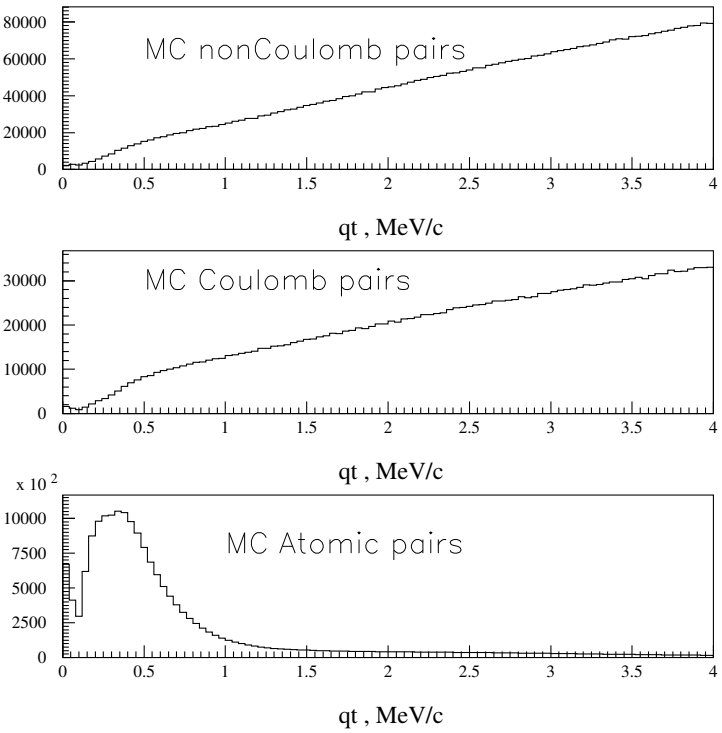

Figure 11: *Distributions of reconstructed values of Q_t for non-Coulomb, Coulomb pairs and pairs from metastable atom.*

8 Simulation of long-lived $A_{2\pi}$ observation

To evaluate the necessary running time for the observation of long-lived $A_{2\pi}$, the simulation of "experimental data" has been performed adding the contributions of simulated : atomic pairs from long-lived atoms produced in the Platinum foil, atomic pairs from the Beryllium target , "Coulomb pairs", "non-Coulomb pairs" and accidentals. The total amount of data and the relative contribution of the different components are obtained from the analysis of the experimental data collected in 2010 with Beryllium target (see section 6).

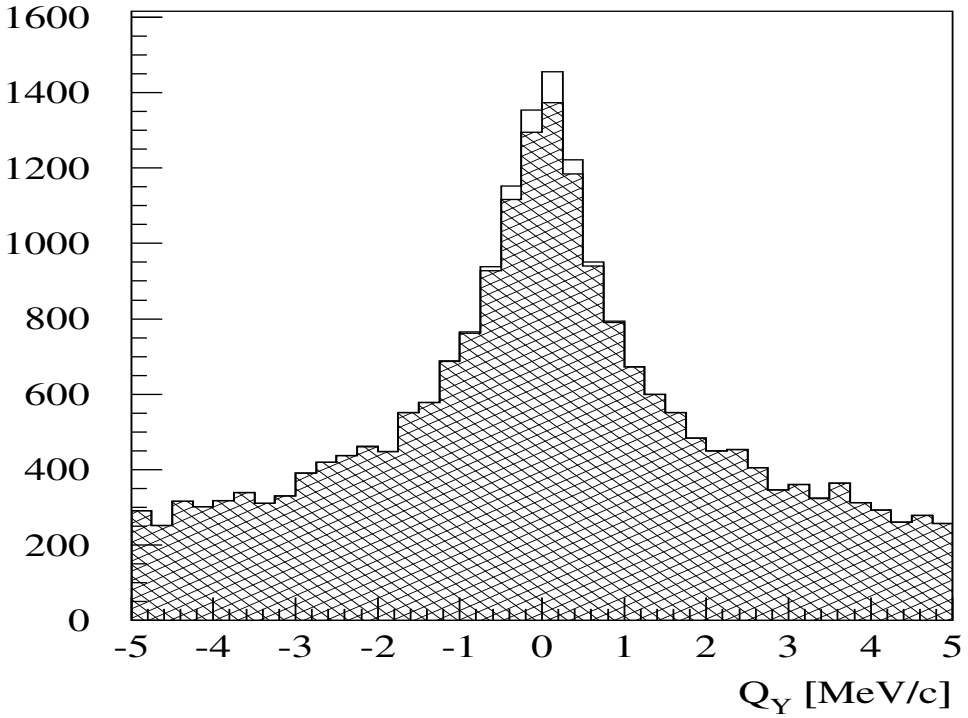

Figure 12: *Simulated distribution of $\pi^+\pi^-$ pairs over Q_Y with criteria: $|Q_X| < 1$ MeV/c, $|Q_L| < 1$ MeV/c. "Atomic pairs" from long-lived atoms (light area) above background produced in Beryllium target (hatched area)*

Fig. 12 presents the distribution of simulated data over the Y projection of relative momentum Q . The cuts on $|Q_X| < 1$ MeV/c and $|Q_L| < 1$ MeV/c have been applied. Simulation shows that in each projection such criterion selects more than 90% of "atomic pairs" from long-lived atoms. Hatched area is a sum of all pairs produced in Beryllium target and light area corresponds to "atomic pairs" from long-lived atoms (broken in the Platinum foil). The signal-to-background ratio is small. It can be improved by installation of an additional retractable magnet which induces the horizontal magnetic field in the gap between Be target and Pt foil. A magnet with the bending power of 0.01 T·m would shift the Q_Y value by 6 MeV/c only for the pairs produced in the Be target leaving unchanged the Q_Y distribution of the pairs produced in the Pt foil. The magnet with such characteristics is already available to be installed (see Fig. 13). Fig. 14 shows the resulting Q_Y distribution with the improved signal-to-background ratio.

A new sample of simulated data with the additional magnet has been fitted with the sum of the distributions of atomic pairs from long-lived atoms, "Coulomb pairs" and "non-Coulomb pairs". The atomic pairs produced in the Be target with the Q_Y about 6 MeV/c are are absent in the fit region. The fitting procedure is the standard one used in DIRAC [ADEV05]. The free parameters in the fit are the

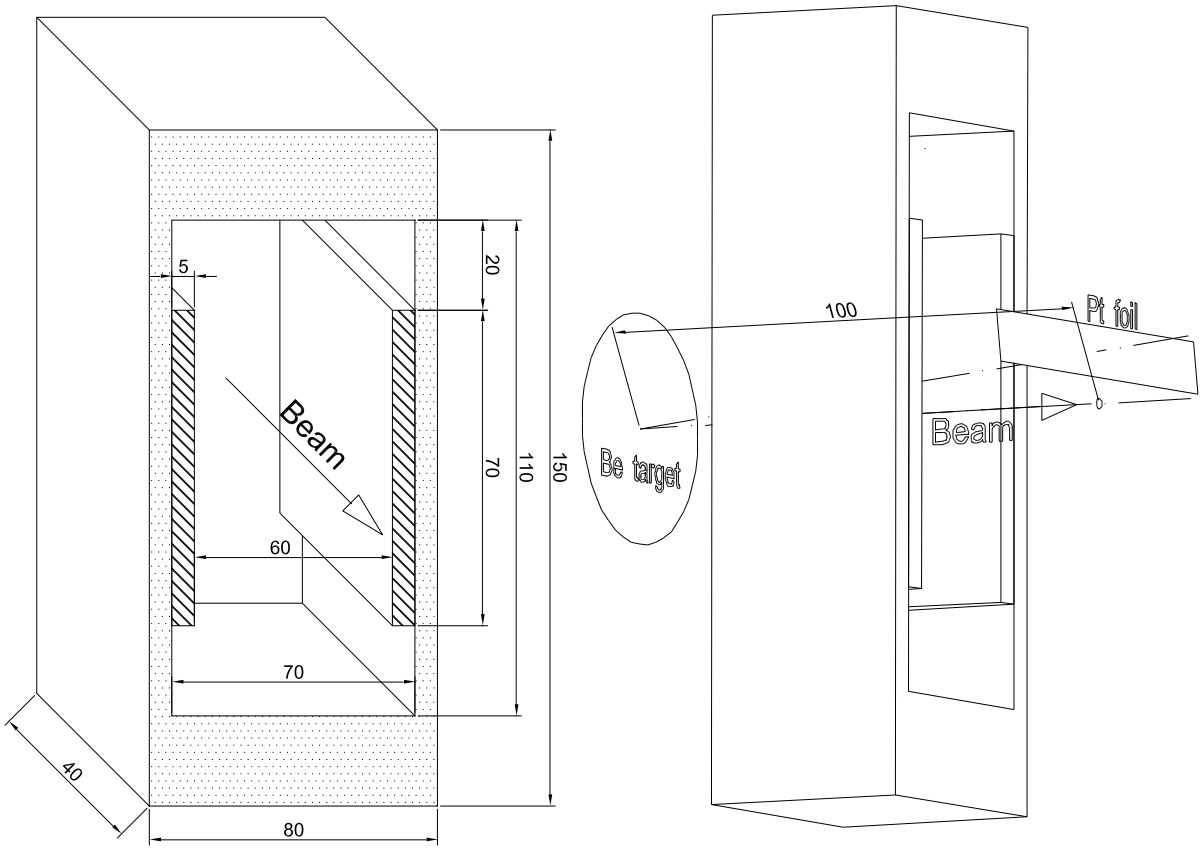

Figure 13: *Permanent magnet dimensions and arrangement of the Beryllium target, permanent magnet and Platinum foil.*

relative amounts of each of the former distributions to the total number of events. The fit results for distribution over Q_L (with cut $Q_T < 1$ MeV/c) are presented in Fig. 15. Number of atomic pairs are found to be:

$$n_A^l = 281 \pm 48$$

Analysis of the experimental data accounting widths of the atomic pairs distribution over different components of the relative momentum Q allows to find the variable F which provides the distribution of atomic pairs with the best signal-to-background ratio:

$$F = \sqrt{\left(\frac{Q_X}{0.50}\right)^2 + \left(\frac{Q_Y}{0.32}\right)^2 + \left(\frac{Q_L}{0.56}\right)^2} \tag{11}$$

Here 0.50, 0.32 and 0.56 in units of Mev/c are RMSs of the atomic pairs distribution over corresponding components of the relative momentum Q.

Fig. 16 presents results of analysis for distribution of $\pi^+\pi^-$ pairs over F. It provides a greater number of found atomic pairs due to the weaker cut on $Q_T < 2$ MeV/c and a better signal-to-error ratio:

$$n_A^l = 327 \pm 37 \tag{12}$$

$$\frac{n_A}{\sigma_{n_A}} = 8.8 \tag{13}$$

It is worth noting that the simulated number n_A^l is 310.

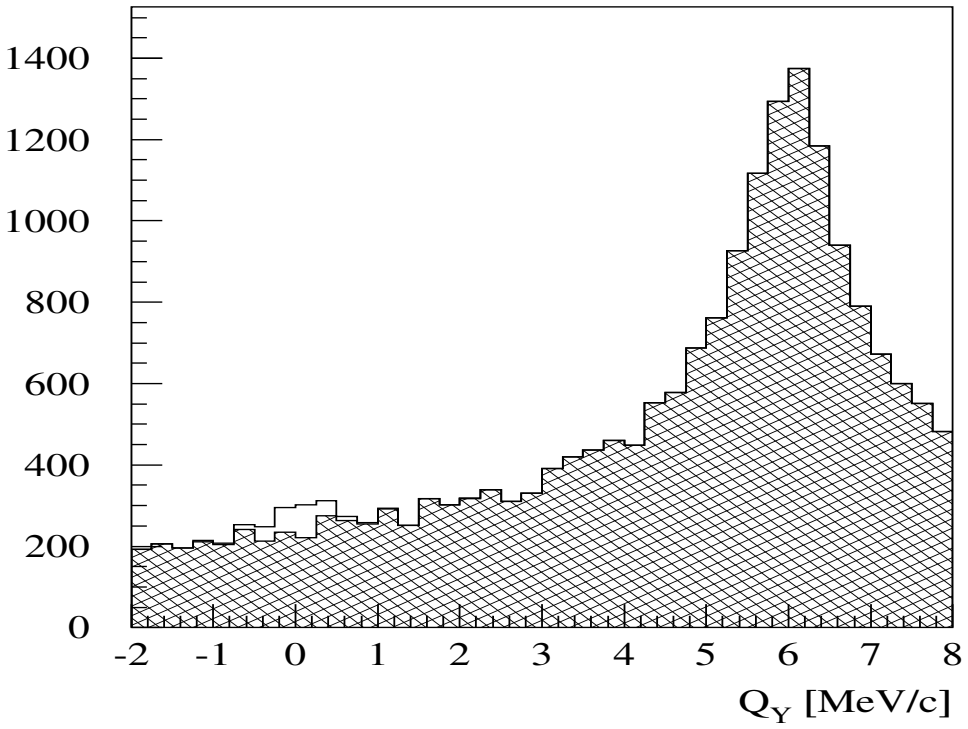

Figure 14: *Simulated distribution of $\pi^+\pi^-$ pairs over Q_Y with criteria: $|Q_X| < 1$ MeV/c, $|Q_L| < 1$ MeV/c. Additional magnet is implemented. "Atomic pairs" from long-lived atoms (light area) above background produced in Beryllium target (hatched area)*

In order to declare an observation of long-lived $A_{2\pi}$ it is needed to achieve a ratio between signal and error greater than 5. The current simulation provide the ratio of 8.8. This means that probability to observe long-lived $A_{2\pi}$ is close to 100%.

An additional simulation with 2 μm Pt foil shows that compared to the 1 μm case the number of reconstructed events increases by factor 1.17 due to the higher probability of atom breakup (see Table 4). However the a higher multiple scattering spreads the signal and increase background below and thus increases the error by factor 1.13. So the final gain in the signal-to-error ratio for 2 μm Pt foil is about 3% compared to 1 μm. An additional decrease in the multiple scattering can be achieved due to extension of the vacuum pipe between the target and forward detectors by 1 meter, that decrease the error in the number of reconstructed events by about 9%.

In the approach without the additional permanent magnet the accuracy of signal separation will be worse. At equal conditions the simulated number of reconstructed atomic pairs is $n_A^l = 334 \pm 89$. To achieve the value of 5 in the signal-to-error ratio, required for the observation, the needed statistic should be increased by 1.8 that can be accomplished with a high efficiency of the event reconstruction and/or a longer run time.

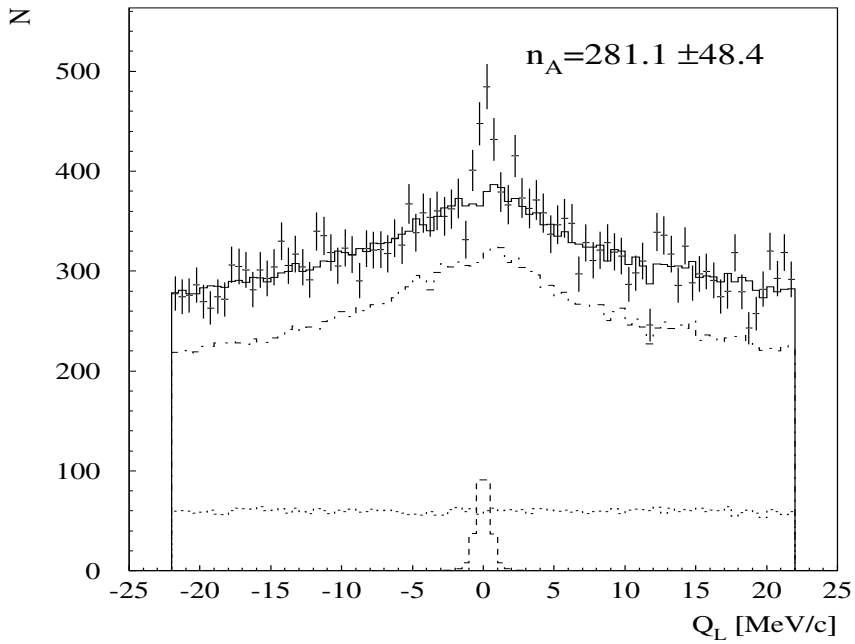

Figure 15: *Simulated distribution of $\pi^+\pi^-$ pairs over Q_L, with criterion Q_T < 1 MeV/c. "Experimental" data (points with error bars) are fitted by a sum of "atomic pairs" from long-lived states (dashed line), "Coulomb pairs" (by dotted-dashed line), "non-Coulomb pairs" (dotted line). The background sum is shown by the solid line.*

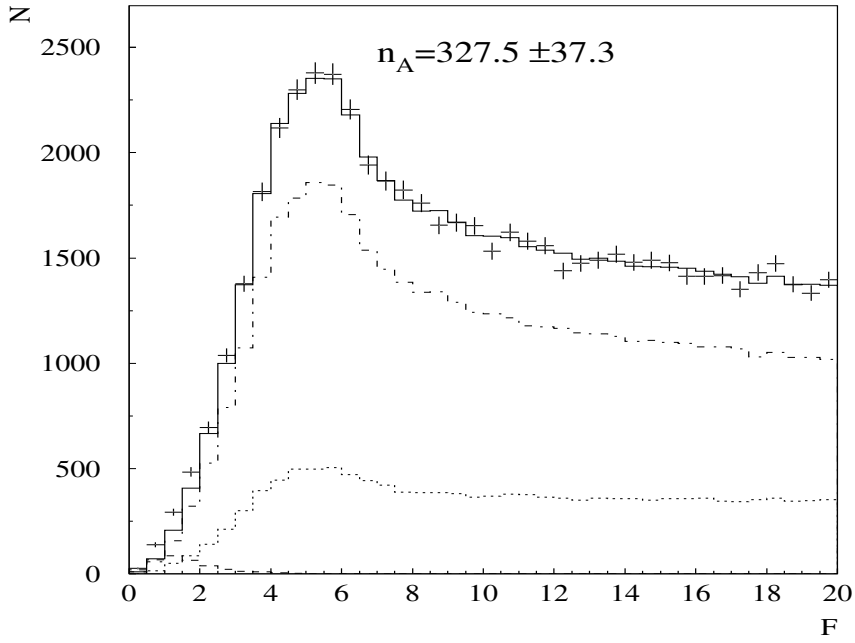

Figure 16: *Simulated distribution of $\pi^+\pi^-$ pairs over F, with criterion Q_T < 2 MeV/c. "Experimental" data (points with error bars) are fitted by a sum of "atomic pairs" from long-lived states (dashed line), "Coulomb pairs" (by dotted-dashed line), "non-Coulomb pairs" (dotted line). The background sum is shown by the solid line.*

9 Measurement of multiple scattering for different materials

In the last DIRAC result (9) [ADEVA11] the statistical and systematic errors in the value of $|a_0 - a_2|$ are of the same magnitude of 3%. With the additional data collected in 2008–2010 the statistical error is expected to be reduced to 2%. So some extra steps should be taken for reducing the systematic error also.

The current value of the systematic error by 80% determine by the accuracy of multiple scattering simulation in the Ni target. The angle of multiple scattering in the Ni target was measured during two months in 2003 in parallel with the ordinary data taking [DUDA08]. The accuracy of this measurement was 1% and mainly determined by the amount of collected data. So repetition of this measurement during 6 months in 2011 in parallel with data taken discussed above will provide enough statistic to reduce the systematic error in the final result to the level lower than statistical one.

Moreover now the data acquisition system allows to collect events with 5 times higher rate compared to 2003. So influence of statistic on the accuracy of the scattering angle measurement will be suppressed significantly. The measurement procedure allows to install few scatterers in parallel. It will permits to estimate systematic error in the angle measurement with scatterer of the same material and to perform measurement with different materials for a precise check of the existing theory of multiple scattering. It is planed to install as the scatterer the Ni target of 100 μm used in 2003–2010 to measure the scattering angle of the specific object. In addition few pieces of Nickel, Beryllium and Platinum foils will be installed.

10 Conclusion

During the short run in 2010 the experimental conditions for observation of the long-lived states of $\pi^+\pi^-$ atoms with Be target were studied. It allowed to optimize the proton beam intensity and collect the data which permitted to obtain the production rates of $A_{2\pi}$ and $\pi^+\pi^-$ pairs of all types. Basing on these experimental data all processes of production and reconstruction of $A_{2\pi}$ with all backgrounds was simulated. This investigation shows that the long-lived states of $\pi^+\pi^-$ atoms can be observed at the level more than 8σ during 6 months of data taken, equivalent to the one in 2010. The required total number of accelerator spills of about $1.1 \cdot 10^6$ is the same as in 2010. The optimal proton beam intensity in the channel is $2.6 \cdot 10^{11}$ proton/spill, that provides the total proton flux through the target of $2.9 \cdot 10^{17}$.

References

[ADEVA11] B. Adeva *et al.*, to be submitted to Phys.Rev.Lett.

[ADEV05] B. Adeva *et al.*, Phys. Lett. B 619 (2005) 50.

[AFAN97] L. G. Afanasyev, "Observation of $\pi^+\pi^-$ atom", PhD thesis, JINR, Dubna, 1997.

[AFAN05] L. Afanasyev, G. Colangelo, J. Schacher, HadAtom05 — Workshop on Hadronic Atoms, February 15–16, 2005, Bern, Switzerland, http://arxiv.org/abs/hep-ph/0508193.

[AUST83] G.J.M.Austen, J.J. de Swart, Phys.Rev.Lett. 50 (1983) 2039.

[BILE69] S.M. Bilenky *et al.*, Yad. Phys. 10 (1969) 812; (Sov. J. Nucl. Phys. 10 (1969) 469).

[BUTT04] P. Buettiker, S. Descotes-Genon, B. Moussallam, Eur. Phys. J. C 33 (2004) 409.

[COLA01B] G. Colangelo, J. Gasser and H. Leutwyler, Nucl. Phys. B603 (2001) 125.

[DESC03] S. Descotes *et al.*, LPT-ORSAY/03-82, ECT*-03-06, IPNO DR 03-09; hep-ph/0311120.

[DESE54] S. Deser *et al.*, Phys. Rev. 96 (1954) 774.

[DUDA08] A. Dudarev, V. Kruglov, L. Kruglova, M. Nikitin, "Pion multiple Coulomb scattering in the DIRAC experiment", DIRAC NOTE 08-06, http://dirac.web.cern.ch/DIRAC/i_notes.html

[EFIM02] G.V. Efimov, M.A. Ivanov and V.E. Lyubovitskij, Yad. Fiz. 44 (1986) 460; (Sov. J. Nucl. Phys. 44 (1986) 296.

[EFIM86] G. V. Efimov, M. A. Ivanov and V. E. Lyubovitskij, Yad. Fiz. 44 (1986) 460; Sov. J. Nucl. Phys. 44 (1986) 296.

[EIRA00] D.Eiras and J.Soto, Phys.Lett. B491 (2000) 101; hep-ph/0005066.

[GASH98] A. Gashi *et al.*, Nucl. Phys. A628 (1998) 101.

[GASS01] J. Gasser *et al.*, Phys.Rev. D64 (2001) 016008; hep-ph/0103157.

[GORC00] O. E. Gorchakov *et al.*, Yad. Fiz. 63 (2000) 1936; (Phys. At. Nucl. 63 (2000) 1847).

[IVAN98] M.A. Ivanov *et al.*Phys. Rev. D58 (1998) 094024.

[JALL98] H. Jallouli and H. Sazdjian, Phys. Rev. D58 (1998) 014011; Erratum: ibid., D58 (1998) 099901.

[KARI79] A. Karimhodjaev and R. N. Faustov, Yad. Fiz. 29 (1979) 463; Sov.J.NuclPhys. 29 (1979) 232.

[LEUT93] H. Leutwyler, Proc. XXVI Int. Conf. on High Energy Physics, Dallas, 1992, edited by J. R. Sanford, IAP Conf. Proc. N.272 (AIP New York 1993) 185.

[NA48-09] J.R. Batley *et al.*, Eur. Phys. J. C 64 (2009) 589–608.

[NA48-10] J.R. Batley *et al.*, Eur. Phys. J. C 70 (2010) 635–657.

[NEME01] L. L. Nemenov and V. D. Ovsyannikov, Phys. Lett. B514 (2001) 247.

[NEME02] L. L. Nemenov, V. D. Ovsyannikov and E. V. Chaplygin, Nucl. Phys. A 710 (2002) 303.

[NEME85] L. L. Nemenov, Yad. Fiz 41 (1985) 980; Sov. J. Nucl. Phys. 41 (1985) 629.

[SCHW04] J. Schweizer, *Phys. Lett. B* 587 (2004) 33, arXiv:hep-ph/0401048;
J. Schweizer, *Eur. Phys. J. C* 36 (2004) 483. arXiv:hep-ph/0405034.

[URET61] J. Uretsky and J. Palfrey, Phys. Rev. 121 (1961) 1798.

[DIPGEN] M.Zhabitsky, DIRAC Note 2007-11.